

# On the glass–crystal transformation kinetics in materials which fulfil the conditions of “site saturation”. Application to the crystallization of some alloys of Sb–As–Se and Ge–Sb–Se glassy systems

J. Vázquez · R. González-Palma · J. L. Cárdenas-Leal ·  
D. García-G. Barreda · P. L. López-Alemaný ·  
P. Villares

Received: 14 October 2009 / Accepted: 3 February 2010 / Published online: 9 March 2010  
© Springer Science+Business Media, LLC 2010

**Abstract** A theoretical procedure has been developed for the kinetic study of the glass–crystal transformation under continuous heating regime in materials involving formation and growth of nuclei. The quoted procedure obtains an evolution equation with the temperature for the actual volume fraction transformed at non-isothermal reactions. In this procedure an extended volume of transformed material has been defined and spatially random transformed regions have been assumed in order to obtain a general expression of the actual volume fraction transformed as a function of the temperature using differential scanning calorimetry. The kinetic parameters of the quoted transformation have been deduced, assuming that the crystal growth rate has an Arrhenius-type temperature dependence, and the nucleation frequency is negligible, condition of “site saturation”, and using the following considerations: the condition of maximum crystallization rate and the quoted maximum rate. The procedure developed has been applied to the analysis of the crystallization kinetics of some semiconducting alloys, prepared in our laboratory, corresponding to the Sb–As–Se and Ge–Sb–Se glassy systems, and which fulfil the condition of “site saturation”. The obtained values for the kinetic parameters satisfactorily agree with the calculated results by the non-isothermal technique of maximum-value. This fact confirms the reliability and accuracy of the theoretical procedure developed.

## Introduction

Although the glass has been used as an artistic medium and industrial material for centuries it has been only in relatively recent years when the “glass science” has emerged as a field of study in its own right. Thus, the knowledge of glassy materials is one of the most active fields of research in the physics of condensed matter today [1], although traditionally, solid-state physics has meant crystal physics, and solidity and crystallinity have been considered as synonymous in texts on condensed matter. Therefore, the solid-state research in recent years has played an important role in the study of solids that are not crystals, solids for which the arrangement of the atoms lacks the slightest vestige of long-range order. The great interest in these materials is largely due to their ever increasing applications in modern technology. Their possibilities in the immediate future are huge based on the characteristic properties such as electronic-excitation phenomena, chemical reactivity and inertia and superconductivity. Therefore, the advances that have been made in the physics and chemistry of the quoted materials, during the last 50 years, have been appreciated within the research community. A strong theoretical and practical interest in the application of isothermal and non-isothermal experimental analysis techniques to the study of phase transformations has arisen in the last decades. In the isothermal regime [2, 3] the glass samples are quickly heated up and held a temperature above glass transition temperature. In this regime, the glasses crystallize a constant temperature. However, in the non-isothermal regime [4–8] the glass samples are heated up at a fixed heating rate. Generally, an isothermal experiment takes longer time than a non-isothermal experiment, but isothermal experimental data can be interpreted by the well-established Johnson–Mehl–Avrami (JMA) kinetic

---

J. Vázquez (✉) · R. González-Palma · J. L. Cárdenas-Leal ·  
D. G.-G. Barreda · P. L. López-Alemaný · P. Villares  
Departamento de Física de la Materia Condensada, Facultad  
de Ciencias, Universidad de Cádiz, Apartado 40,  
11510 Puerto Real, Cádiz, Spain  
e-mail: jose.vazquez@uca.es

equation [9–12]. On the contrary, the non-isothermal experiments have as advantage, the rapidity that makes this type of experiments more attractive. The use of non-isothermal techniques to study solid-state transformations and to determine the kinetic parameters of the rate controlling processes have been increasingly widespread. Therefore, the consideration of the non-isothermal regime has produced a large number of mathematical treatments for analysing thermal process data, the most of the quoted treatments are based on the JMA transformation rate equation [9–12]. Thus, many authors have used the so called Kissinger plot [13] or Ozawa plot [14] directly to examine the crystallization kinetics of amorphous materials. However, these methods, cannot be directly applied to the crystallization of amorphous materials and the physical meaning of the activation energies, thus obtained, can be obscure because the crystallization is advanced not by the *n*th order reaction but by the nucleation and growth process [15]. On the other hand, some authors applied the JMA equation to the non-isothermal crystallization processes [16–18]. Although sometimes they appeared to get reasonable activation energies, this procedure is not appropriate because the quoted equation strictly applies only to isothermal experiments [19]. In the present article, a theoretical procedure has been developed to obtain an evolution equation with the temperature for the actual volume fraction transformed at non-isothermal reactions in materials involving formation and growth nuclei. In the quoted procedure an extended volume of transformed material has been defined and spatially random transformed regions have been assumed in order to obtain a general expression of the actual fraction transformed as a function of the temperature. The kinetic parameters of the glass–crystal transformation, by using differential scanning calorimetry (DSC), have been deduced by means of the following considerations: the condition of maximum crystallization rate and the quoted maximum rate. Moreover, the present work applies the developed procedure to the crystallization kinetics of the glassy alloys: Sb<sub>0.08</sub>As<sub>0.44</sub>Se<sub>0.48</sub> (S1), Sb<sub>0.12</sub>As<sub>0.40</sub>Se<sub>0.48</sub> (S2) and Ge<sub>0.13</sub>Sb<sub>0.23</sub>Se<sub>0.64</sub> (S3), prepared in our laboratory, as-quenched and previously reheated. In accordance with the corresponding results, it is possible to establish that in the considered alloys the nuclei were dominant before the thermal treatment, and because of it the reheating does not change in a considerable way the number of the pre-existing nuclei in the quoted alloys, which fulfil the condition of “site saturation” [20, 21]. We have confirmed this condition checking that the kinetic exponent, *n*, is maintained constant after the reheating for the three alloys analysed, as it is described in the literature [22]. Finally, the obtained values for the kinetic parameters by means of the developed procedure are compared with the corresponding results calculated by the

maximum-value technique, finding that the error between them for the less accurate parameter is less than 6.8%. This fact shows the reliability and accuracy of the theoretical procedure developed.

### Basic theory

#### Deducing the volume fraction transformed

The theoretical basis for interpreting DSC results is provided by the formal theory of transformation kinetics [9–13, 23, 24]. This formal theory supposes that the crystal growth rate, in general, is anisotropic. This rate in any direction can be then represented in terms of the principal growth velocities, *u<sub>i</sub>(t)* (*i* = 1, 2, 3), in three mutually perpendicular directions, and therefore, the volume of a region originating at time *t* = τ (τ being the nucleation period) is then

$$v_\tau = g \prod_i \int_{(1-\alpha)\tau}^t u_i(t') dt' \tag{1}$$

where the expression  $\prod_i \int_{(1-\alpha)\tau}^t u_i(t') dt'$  condenses the product of the integrals corresponding to the values of the above quoted subscript *i*, α is a parameter equal to zero in the case of continuous nucleation and equal to the unit in the case of “site saturation” [20, 21], and finally, *g* is a geometric factor, which depends on the dimensionality and shape of the crystal growth, and therefore its dimension equation can be expressed as

$$[g] = [L]^{3-i} \text{ ([L] is the length).}$$

Defining an extended volume, *V<sub>e</sub>*, of transformed material and assuming spatially random transformed regions [5, 25, 26], the elemental extended volume, *dV<sub>e</sub>*, is written as

$$dV_e = v_\tau V dN = gV \left[ \prod_i \int_{(1-\alpha)\tau}^t u_i(t') dt' \right] dN \tag{2}$$

where *dN* is the number of nuclei existing in a volume element of material and *V* is the volume of the whole assembly. In accordance with the literature [27], it is possible to write a relation between the elemental true volume, *dV<sub>b</sub>*, and the elemental extended volume, *dV<sub>e</sub>*, in the form

$$dV_b = \left( 1 - \frac{V_b}{V} \right) dV_e = (1 - x) dV_e \tag{3}$$

where *x* = *V<sub>b</sub>*/*V* is the volume fraction transformed. Differentiating this expression and combining Eqs. 2 and 3, one obtains

$$\frac{dx}{1-x} = g \left[ \prod_i \int_{(1-x)\tau}^t u_i(t') dt' \right] dN \tag{4}$$

When the crystal growth rate is isotropic,  $u_i = u$ , an assumption, which is in agreement with the experimental evidence, since in many transformations the reaction product grows approximately as spherical nodules [27], Eq. 4 can be written as

$$\frac{dx}{1-x} = g \left[ \int_{(1-x)\tau}^t u(t') dt' \right]^m dN \tag{5}$$

where  $m$  is an exponent related to the dimensionality of the crystal growth and the mode of transformation.

It should be noted that for continuous nucleation the above-mentioned number of nuclei,  $dN$ , in terms of the nucleation frequency per unit volume,  $I_v(\tau)$ , is written as  $dN = I_v(\tau)d\tau$  and Eq. 5 becomes

$$\frac{dx}{1-x} = g I_v(\tau) \left[ \int_{\tau}^t u(t') dt' \right]^m d\tau \tag{6}$$

whereas for “site saturation” Eq. 5 is written as

$$\frac{dx}{1-x} = g \left[ \int_0^t u(t') dt' \right]^m dN \tag{7}$$

In non-isothermal crystallization experiments with a quenched glass containing no nuclei and assuming that the nucleation frequency is practically constant and crystal growth rate has an Arrhenian temperature dependence,  $u = u_0 \exp(-E/RT)$ ,  $E$  being the activation energy of the process Eq. 6 becomes

$$\frac{dx}{1-x} = \frac{g I_v u_0^m}{\beta^m} \left\{ \int_{T_\tau}^T [\exp(-E/RT')] dT' \right\}^m d\tau = \frac{C_1}{\beta^m} I_v I_1^m d\tau \tag{8}$$

where  $T_\tau$  is the corresponding temperature at time  $\tau$  and  $\beta = dT/dt$  is the heating rate.

Using the substitution  $y' = E/RT'$ , the integral  $I_1$  is transformed in an exponential integral of order two, which can be expressed, in accordance with the literature [28], by the alternating series

$$S_2(y, y_\tau) = \left[ \frac{-e^{-y'}}{y'^2} \sum_{k=0}^{\infty} \frac{(-1)^k (k+1)!}{y'^k} \right]_{y_\tau}^y \tag{9}$$

Considering that in this type of series the error produced is less than the first term neglected and bearing in mind that in most crystallization reactions  $y' = E/RT' \gg 1$ , usually

$E/RT' \geq 25$  [26], it is possible to use only the first term of the series, without making any appreciable error. Moreover, given that  $T > T_\tau$  and therefore,  $y_\tau = qy$  with  $q > 1$ , the integral  $I_1$  can be expressed as

$$I_1 = \frac{E}{R} \left( \frac{e^{-y'}}{y'^2} \right)_{y_\tau}^y = \frac{E e^{-y}}{R y^2} [1 - q^{-2} e^{-(q-1)y}] = \frac{E e^{-y}}{R y^2} (1 - Q) \tag{10}$$

Bearing in mind that  $y \gg 1$  and  $e^{-(q-1)y} \ll 1$ , the term  $Q$  is negligible in comparison with the unit and Eq. 10 becomes

$$I_1 = \frac{E e^{-y}}{R y^2}. \tag{11}$$

The logarithm of the expression  $e^{-y}y^{-2}$  leads to an expression that, in the range of values of  $y$ ,  $20 < y < 60$ , can be fitted very satisfactorily by a linear approximation, giving

$$\ln(e^{-y}y^{-2}) = -5.1222 - 1.053y \tag{12}$$

and therefore

$$I_1 \approx (E/R) e^{-5.1222} e^{-1.053y} = A_1 e^{-1.053E/RT} \tag{13}$$

To illustrate the above-mentioned fit, Fig. 1 shows the points  $(y, \ln(e^{-y}y^{-2}))$  together with the corresponding straight regression line.

Substituting Eq. 13 into Eq. 8 and integrating the resulting expression one obtains

$$\begin{aligned} -\ln(1-x) &= \frac{C_2}{\beta^{m+1}} I_v (T - T_0) \exp(-1.053mE/RT) \\ &= \frac{C_2 N_0}{\beta^{m+1}} \exp(-1.053mE/RT) \end{aligned} \tag{14}$$

$N_0$  being the nuclei formed per unit volume in the course of the thermal process at the heating rate  $\beta$ .

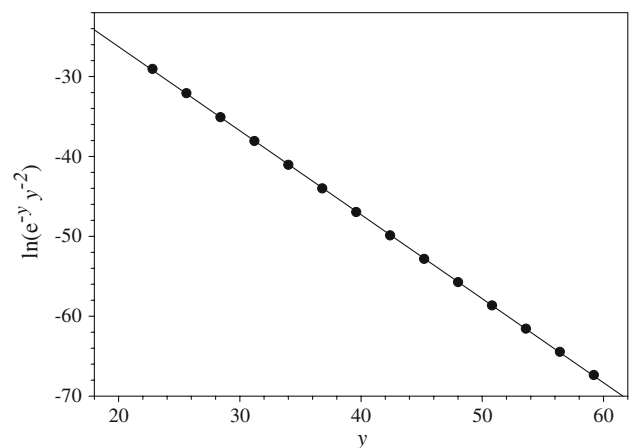


**Fig. 1** Representation of  $\ln(e^{-y}y^{-2})$  vs.  $y$  and corresponding straight regression line for the range of values  $20 < y < 60$

In the case of a glass which has been previously heated at the temperature of maximum nucleation rate for sufficiently long time, a large number of nuclei already exist and no new nuclei are formed during the thermal process “site saturation” [20, 21] (i.e.  $I_V = 0$ ), Eq. 7 can be written as

$$\frac{dx}{1-x} = \frac{C_1}{\beta^m} \left[ \int_{T_0}^T \exp(-E/RT') dT' \right]^m dN = \frac{C_1 I_2^m}{\beta^m} dN \quad (15)$$

The integral  $I_2$  is evaluated in the same manner as  $I_1$ , and substituting the resulting expression into Eq. 15 yields

$$\frac{dx}{1-x} = \frac{C_2 N}{\beta^m} \exp(-1.053mE/RT) dN$$

and therefore

$$-\ln(1-x) = \frac{C_2 N}{\beta^m} \exp(-1.053mE/RT) \quad (16)$$

Equations 14 and 16 may be expressed by the more general relationship

$$-\ln(1-x) = \frac{C_0}{\beta^n} \exp(-1.053mE/RT) \quad (17)$$

corresponding to the evolution with the temperature of the actual volume fraction transformed.

According to the literature [22],  $n = m + 1$  for a quenched glass containing no nuclei and  $n = m$  for a glass containing a sufficiently large number of nuclei. For diffusion-controlled growth with  $u$  independent of time,  $m$  assumes the values 1, 2 and 3 for one-, two- and three-dimensional growth, respectively.

### Calculating kinetic parameters

The usual analytical methods, proposed in the literature for analyzing the crystallization kinetics in the glass forming liquids, assume that the reaction rate constant can be defined by an Arrhenian temperature dependence. In order to this assumption to hold, one of the following two sets of conditions should apply [26]:

- (i) The crystal growth rate,  $u$ , has an Arrhenian temperature dependence; and over the temperature range where the thermoanalytical measurements are carried out the nucleation rate is either constant or negligibly.
- (ii) Both the crystal growth rate and the nucleation frequency have Arrhenian temperature dependences.

In the present work the first condition is assumed, and the crystallization rate is obtained by deriving the actual volume fraction transformed with respect to time, and from the Eq. 17 results in:

$$\frac{dx}{dt} = \frac{C_0}{\beta^{n-1}} (1-x) \frac{1.053mE}{RT^2} \exp(-1.053mE/RT). \quad (18)$$

The maximum crystallization rate is found by making  $d^2x/dt^2 = 0$ , thus obtaining the relationship

$$\left( \frac{dx}{dt} \right) \Big|_p = (1-x_p) \left\{ T_p^2 \left[ \frac{d}{dt} \left( \frac{1}{T^2} \right) \right] \Big|_p + 1.053mE\beta / RT_p^2 \right\} \quad (19)$$

where the subscript  $p$  denotes the quantity values corresponding to the maximum crystallization rate.

Taking a sufficiently limited range of temperature (such as the range of crystallization peaks in DSC experiments), the fraction  $1/T^2$  can be considered practically constant, and therefore Eqs. 18 and 19 become, respectively

$$\left( \frac{dx}{dt} \right) \Big|_p = K_1 \beta^{-(n-1)} (1-x_p) \exp(-1.053mE/RT_p) \quad (20)$$

and

$$\left( \frac{dx}{dt} \right) \Big|_p = 1.053mE\beta(1-x_p) / RT_p^2 \quad (21)$$

Relating to Eqs. 20 and 21 and taking the logarithm leads to the relationship

$$\ln \left( T_p^2 / \beta^n \right) = \frac{1.053mE}{R} \frac{1}{T_p} + \text{constant} \quad (22)$$

which represents a straight line whose slope yields the product  $mE$  of the crystallization process.

The use of Eq. 22 implies a previous knowledge of the kinetic exponent,  $n$ , which can be obtained taking the logarithm of Eq. 17, yielding

$$z = \ln[-\ln(1-x)] = -n \ln \beta - 1.053mE/RT + \ln C_0 \quad (23)$$

and representing  $z$  versus  $\ln \beta$  at a fixed temperature.

The  $m$ -value should also be known, a parameter that depends on the dimensionality of the crystal. One method for determining the  $m$ -value is to observe the change of  $n$  with reheating at the nucleation temperature (slightly higher than the glass transition temperature,  $T_g$ ). If  $n$  does not change with reheating, a large number of nuclei already exists in the specimen and  $n = m$ . If  $n$  decreases with reheating, not so many nuclei exist in the specimen. In this case,  $m < n \leq m + 1$  before reheating and  $n = m$  after reheating [22].

Once the crystallization mechanism is precisely known and does not change with the heating rate, the plot of  $\ln(T_p^2/\beta^n)$  vs.  $1/T_p$  gives the above-mentioned value of  $mE$ . Dividing  $mE$  by  $m$ , the activation energy for the transformation can be obtained.

Finally, it should be noted that the change of  $\ln(T_p^2)$  with  $\beta$  is negligibly small compared with the change of  $\ln(\beta^n)$ , and, therefore, it is possible to write

$$\ln(\beta^n) = -\frac{1.053mE}{R} \frac{1}{T_p} + \text{constant} \quad (24)$$

expression often used to obtain the activation energy.

## Experimental procedures

In this section, the preparation and the thermal treatment of the glassy alloy S2 is described as an illustrative example of the alloys analysed in the present work and obtained in our laboratory. The  $\text{Sb}_{0.12}\text{As}_{0.40}\text{Se}_{0.48}$  glassy semiconductor was made in bulk form, from their components of 99.999% purity, which were pulverized to less than 64  $\mu\text{m}$ , mixed in adequate proportions, and introduced into quartz ampoules. The ampoules were subjected to an alternating process of filling and vacuuming of inert gas, in order to ensure the absence of oxygen inside. This ended with a final vacuuming process of up to  $10^{-2}$  Pa, and sealing with an oxyacetylene burner. The ampoules were put into a furnace at 1,223 K for 44 h, turning at 1/3 rpm, in order to ensure the homogeneity of the molten material, and then quenched in water with ice to avoid the crystallization. The capsules containing the samples were then put into a mixture of hydrofluoric acid and hydrogen peroxide in order to corrode the quartz and make it easier to extract the alloy. The glassy state of the material was confirmed by a diffractometric X-ray scan, in a Siemens D500 diffractometer, showing an absence of the peaks which are characteristic of crystalline phases. The homogeneity and composition of the samples were verified through scanning electron microscopy (SEM) in a Jeol scanning microscope JSM-820. The calorimetric measurements were carried out in a Perkin-Elmer DSC7 differential scanning calorimeter with an accuracy of  $\pm 0.1$  K. A constant 60  $\text{mL min}^{-1}$  flow of nitrogen was maintained in order to provide a constant thermal blanket within the DSC cell, thus eliminating thermal gradients and ensuring the validity of the applied calibration standard from sample to sample. The calorimeter was calibrated, for each heating rate, using the well-known melting temperatures and melting enthalpies of high purity zinc and indium supplied with the instrument. The analysed samples were crimped into aluminium pans, and their masses were kept about 20 mg. An empty aluminium pan was used as reference. The crystallization experiments were carried out through continuous heating at rates,  $\beta$ , of 2, 4, 8, 16, 32 and 64  $\text{K min}^{-1}$ . The glass transition temperature was considered as a temperature corresponding to the inflection point of the lambda-like trace on the DSC scan as shown in Fig. 2. The crystallized fraction,  $x$ , at any

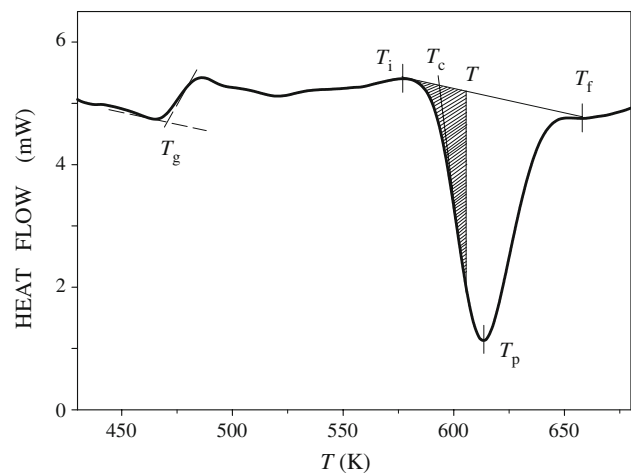


**Fig. 2** Typical DSC trace of  $\text{Sb}_{0.12}\text{As}_{0.40}\text{Se}_{0.48}$  glassy alloy at a heating rate of  $16 \text{ K min}^{-1}$ . The hatched area shows  $A_T$ , the area between  $T_i$  and  $T$

temperature,  $T$ , is given by  $x = A_T/A$ , where  $A$  is the total area limited by the exotherm, between the temperature  $T_i$  where the crystallization is just beginning, and the temperature  $T_f$  where the crystallization is completed and  $A_T$  is the area between the initial temperature and a generic temperature  $T$ , see Fig. 2.

## Results

Following with the alloy taken as an example, the typical DSC trace of the  $\text{Sb}_{0.12}\text{As}_{0.40}\text{Se}_{0.48}$  chalcogenide glass obtained at a heating rate of  $16 \text{ K min}^{-1}$  and plotted in Fig. 2, shows three characteristic phenomena, which are resolved in the temperature region studied. The first one ( $T = 470.0 \text{ K}$ ) correspond to the glass transition temperature,  $T_g$ , the second ( $T = 592.4 \text{ K}$ ) to the extrapolated onset crystallization temperature,  $T_c$ , and the third ( $T = 613.9 \text{ K}$ ) to the peak temperature of crystallization,  $T_p$ , of the above-mentioned chalcogenide glass. It should be noted that the crystallization onset temperature has been extrapolated by using the intersection of the baseline  $T_i$   $T_f$  with the tangent in the inflection point of the transformation exothermal peak (see Fig. 2). The quoted DSC trace shows the typical behaviour of a glass–crystal transformation. The thermograms for the different heating rates,  $\beta$ , quoted in section “Experimental procedures”, show values of the quantities  $T_g$ ,  $T_c$  and  $T_p$  which increase with increasing  $\beta$ , a property which has been widely quoted in literature [29, 30].

### Glass–crystal transformation

The analysis of the glass–crystal transformation kinetics is related to the knowledge of the reaction rate constant as a

function of the temperature. This temperature dependence can be considered of an Arrhenius type when a sufficiently limited range of temperature is used (such as the range of transformation peaks in DSC experiments) [26]. In the present work, given that we have confirmed the condition of “site saturation” of the three alloys analysed, as we afterwards describe in this section, it is considered that the crystal growth rate,  $u$ , has an Arrhenian temperature dependence and over the temperature range where the thermoanalytical measurements are carried out, the nucleation rate is negligible. Accordingly, the crystallization kinetics of the quoted alloys in section “Introduction” may be studied according to the described procedure in the preceding theoretical sections.

With the aim of analyzing the above-mentioned kinetics, the variation intervals of the quantities described by the thermograms of the alloys considered for the different heating rates quoted in section “Experimental procedures”, are given in Table 1, where  $T_i$  and  $T_p$  are the temperatures at which crystallization begins and that corresponding to the maximum crystallization rate, respectively, and  $\Delta T$  is the width of the transformation peak, which is defined as the difference of temperature  $T_f - T_i$  (see Fig. 2). The interval of the crystallization enthalpy,  $\Delta H$ , is also given for each alloy.

The area limited by the exothermal peak of the DSC curve is directly proportional to the total amount of material transformed. The quotient between the ordinates and the total area of the peak gives the corresponding transformation rates, which allow to plot the curves of the exothermal peaks represented in Fig. 3 for the S2 alloy. The precise meaning of  $(dx/dt)_p$  is the maximum-value of the transformation rate (derivative of the volume fraction transformed with respect to time) and it may be observed that the quoted value increases in the same proportion as the heating rate, a property which has been widely discussed in the literature [29, 30].

With the aim of correctly applying the preceding theory each alloy considered was reheated up to a temperature slightly higher than the corresponding  $T_g$  (503 K for S1, 536 K for S2 and 543 K for S3) during the necessary time

**Table 1** Characteristic temperatures and enthalpies of the crystallization processes of the studied alloys

Quantity	Experimental value		
	S1	S2	S3
$T_g$ (K)	457.6–482.6	459.2–490.9	474.3–499.2
$T_i$ (K)	528.6–567.1	553.7–598.8	558.7–599.7
$T_p$ (K)	549.4–596.2	579.3–641.4	581.1–631.3
$\Delta T$ (K)	35.6–49.3	51.2–73.0	42.2–60.2
$\Delta H$ (mcal mg <sup>-1</sup> )	3.7–4.9	2.9–6.6	6.2–7.7

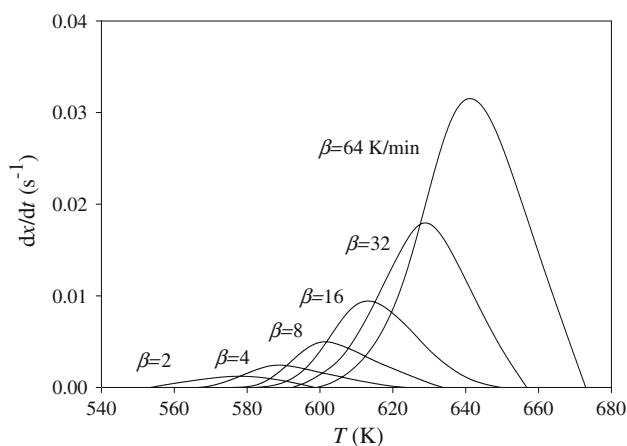


**Fig. 3** Crystallization rate vs. temperature of the exothermal peaks, at different heating rates

in order to form a large number of nuclei. It is ascertained by X-ray diffraction the absence of crystalline peaks at all alloys studied after the nucleation treatment. From the experimental data the plots of  $z = \ln[-\ln(1 - x)]$  vs.  $\ln \beta$ , Eq. 23, at different fixed temperatures have been drawn, both for the as-quenched glasses and for the reheated glasses. It has been observed that the correlation coefficients,  $r$ , of the corresponding straight regression lines, SRL, show a maximum-value for a given temperature, which has been considered as the most adequate one for the calculation of parameter  $n$  for each alloy. The quoted fixed temperatures, the corresponding  $r$ -values and the values of kinetic parameter,  $n$ , for the three alloys analysed both as-quenched and reheated are given in Table 2. Allowing for experimental error, both values of  $n$  parameter for the alloys S1, S2 and S3 are close to 3, 2 and 2, respectively. This indicates that a large number of nuclei exists already in these materials, and therefore the values of the  $m$ -exponent are 3, 2 and 2 for the above quoted alloys, this is, the crystal particles grow three- and two-dimensionally. Accordingly, the three alloys considered fulfil the condition of “site saturation”. As an illustrative example Fig. 4 shows the relation between  $z$  and  $\ln \beta$  for the S2 alloy both as-quenched and reheated at fixed temperatures of 601.4 and 579.3 K, respectively.

**Table 2** Fixed temperatures corresponding to the plots  $\ln[-\ln(1 - x)]$  vs.  $\ln \beta$  with the maximum  $r$ -values and parameter  $n$  for the three alloys studied

Alloy	As-quenched			Reheated		
	$T$ (K)	$r$	$n$	$T$ (K)	$r$	$n$
S1	564.5	0.9997	2.9	561.1	0.9984	2.7
S2	601.4	0.9973	2.0	579.3	0.9997	1.9
S3	604.4	0.9999	2.4	598.8	0.9998	1.9

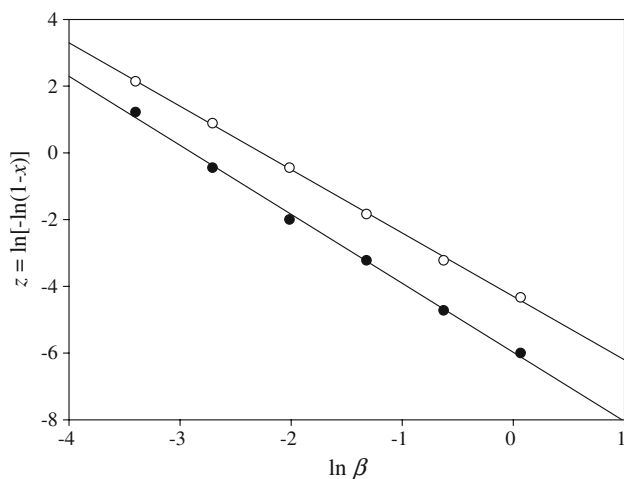


**Fig. 4** Variation of  $\ln[-\ln(1-x)]$  with logarithm of heating rate for S2 alloy ( $\beta$  in  $\text{K s}^{-1}$ ): filled circle, as-quenched glass, 601.4 K; open circle, reheated glass, 579.3 K

It should be noted that once the values of the dimensionality,  $m$ , and of the kinetic exponent,  $n$ , are known for the three alloys considered, according to Eq. 22 it is possible to plot the straight regression lines corresponding to the variation of  $\ln(T_p^2/\beta^n)$  with the reciprocal of the peak temperature, as it is shown in Fig. 5 for the S2 alloy. The values of the activation energy for the crystal growth of the above-mentioned alloys both as-quenched and reheated are obtained from the slopes of the quoted straight lines and given in Table 3. Moreover, we have calculated the values of the mentioned energy using Eq. 24 and the results are also given in Table 3. It should be noted that the values obtained from Eqs. 22 and 24 are very similar, which experimentally demonstrates that the change of  $\ln T_p^2$  with  $\beta$  is negligibly small compared with the change of  $\ln \beta$  in accordance with the literature [26].

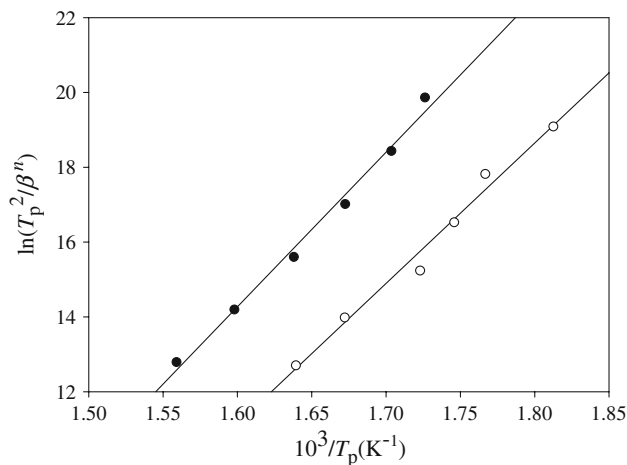


**Fig. 5** Experimental plots of  $\ln(T_p^2/\beta^n)$  vs.  $10^3/T_p$  and straight regression lines of  $\text{Sb}_{0.12}\text{As}_{0.40}\text{Se}_{0.48}$  alloy ( $\beta$  in  $\text{K s}^{-1}$ ): filled circle, as-quenched glass; open circle, reheated glass

On the other hand, from Eq. 23 making explicit the quantity  $\ln \beta$  one obtains an expression, which allows the representation of the above-mentioned quantity versus  $1/T$  for a fixed value of the volume fraction transformed,  $x$ , as it is shown in Fig. 6 for the S2 alloy, when  $x$  is equal to 0.3 and 0.7. Bearing in mind that the quoted expression for a fixed  $x$ -value represents a straight line, it is possible to obtain from the slope the  $E$ -values both for as-quenched glass and for reheated glass, corresponding to the three alloys studied, which are shown in Table 4. Besides, the above-mentioned expression allows to establish a relation between  $\ln \beta$  and  $1/T_p$ ,  $T_p$  being the temperature corresponding to the maximum crystallization rate, already quoted. Since the volume fraction transformed at  $T_p$  is practically constant irrespective of the  $\beta$  value, we include also in Table 4 the values of the activation energy obtained from the slopes of the straight lines  $\ln \beta$  vs.  $1/T_p$  for the three alloys analysed both as-quenched and reheated. It can be observed that the activation energies for the as-quenched alloys, given in Tables 3 and 4 differ by only about 5.8%, which confirms that a large number of nuclei already exists in each as-quenched material studied. Although it might be expected that the activation energy for the crystal growth would be less than the activation energy for the overall crystallization process, for the purpose of the quoted alloys, the values obtained for the parameter  $n$  indicate that the reheating did not cause the appearance of nuclei but that these quenched alloys already contain a sufficient number of nuclei, so that both energies can be mutually identified, because the crystallization process is basically a growth of the pre-existing nuclei.

With the aim of correctly analyzing the reliability of the theoretical procedure described, when a glass–crystal transformation under condition of “site saturation” is studied, we have also applied the maximum-value technique to obtain the kinetic parameters  $E$  and  $n$  of the three semiconducting alloys considered. In the quoted technique, according to the literature [13, 31], the following equations

$$\ln\left(\frac{T_p^2}{\beta}\right) = \frac{E}{RT_p} - \ln\frac{RK_0}{E} \quad (25)$$

and

$$n = \left(\frac{dx}{dt}\right)\bigg|_p RT_p^2 (0.37\beta E)^{-1} \quad (26)$$

allow to obtain the quoted parameters, by using the experimental data: maximum transformation rate,  $(dx/dt)|_p$ , and corresponding temperature,  $T_p$ , to each heating rate. Thus, the activation energy is obtained from the slope of Eq. 25, and the kinetic exponent from Eq. 26. As an example of application of the above-mentioned technique we put forward the case of S2 alloy. In this sense, the experimental

**Table 3** Activation energy obtained from the plots of  $\ln(T_p^2/\beta^n)$  vs.  $T_p^{-1}$  and of  $\ln \beta^n$  vs.  $T_p^{-1}$  for the studied alloys both as-quenched and reheated

Alloy	$E$ (kcal mol <sup>-1</sup> ) using $\ln(T_p^2/\beta^n)$ vs. $T_p^{-1}$		$E$ (kcal mol <sup>-1</sup> ) using $\ln \beta^n$ vs. $T_p^{-1}$	
	As-quenched	Reheated	As-quenched	Reheated
S1	40.5	39.7	41.2	40.4
S2	38.0	37.4	38.5	38.7
S3	46.8	48.2	47.7	49.4

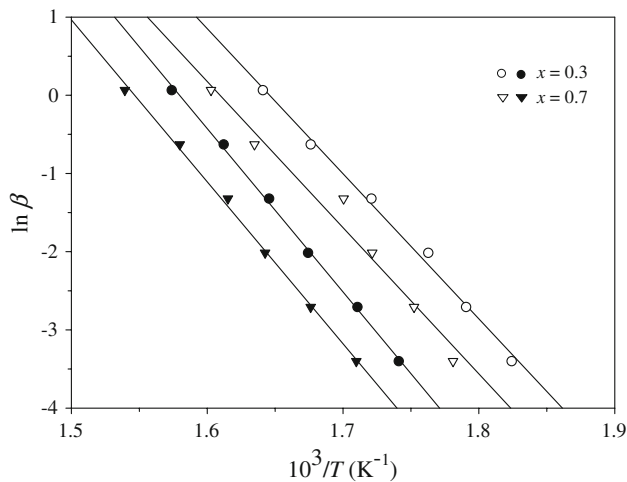


**Fig. 6** Plots of  $\ln \beta$  vs.  $10^3/T$  for the values of the fraction crystallized equal to 0.3 and 0.7 ( $\beta$  in  $K s^{-1}$ ): filled circle, as-quenched glass; open circle, reheated glass

values of the quantities  $T_p$  and  $(dx/dt)|_p$  for the different heating rates, together with the calculated values for the kinetic parameters  $E$  and  $n$  are given in Table 5. The plots of  $\ln(T_p^2/\beta)$  vs.  $1/T_p$  for each heating rate, and the straight regression line carried out for the S2 alloy are shown in Fig. 7. It should be noted that the correlation coefficient of the corresponding fitting is  $r = 0.995$ . The kinetic parameters of the alloys S1 and S3 have been obtained of similar way by mean of the maximum-value technique. Finally, the above-mentioned parameters  $E$  and  $n$ , calculated by means of the quoted theoretical procedure, are compared with its values obtained through the maximum-value technique, Table 6, finding that the error between them for the less accurate parameter is less than 6.8%. This result is in

**Table 5** Kinetic parameters obtained for the crystallization of the S2 alloy using the maximum-value technique

$\beta$ (K min <sup>-1</sup> )	$T_p$ (K)	$10^3 (dx/dt) _p$ (s <sup>-1</sup> )	$n$	$\langle n \rangle$	$E$ (kcal mol <sup>-1</sup> )
2	579.3	1.37	1.96		
4	587.0	2.48	1.82		
8	597.9	5.18	1.97		
16	610.5	9.81	1.95	1.90	38.1
32	625.8	18.26	1.90		
64	641.4	32.43	1.77		

agreement with the literature [26, 32], where it is shown that for  $(n - 1)/n = 0.6$  in the range of  $0.2 < x < 0.7$  it results in an error of 7% in the calculated slope,  $E/R$ , an error acceptable in most crystallization reactions. The quoted fact also confirms that the theoretical procedure developed is adequate to describe the crystallization kinetics of the glassy alloys, which fulfil the condition of “site saturation”.

**Conclusions**

The theoretical procedure described enables us to study the crystallization kinetics in materials involving nucleation and crystal growth processes, which occur in separate stages. This procedure assumes the concept of extended volume in the transformed material and the condition of random nucleation. Using these assumptions we have obtained a general expression for the actual volume fraction transformed as a function of the temperature. In the quoted expression the numerical parameters  $n$  and  $m$

**Table 4** Activation energy obtained from the plot of  $\ln \beta$  vs.  $T^{-1}$  for fixed values of the volume fraction crystallized corresponding to the three alloys analysed

Volume fraction crystallized	$E$ (kcal mol <sup>-1</sup> )					
	S1		S2		S3	
	As-quenched	Reheated	As-quenched	Reheated	As-quenched	Reheated
0.3	43.0	39.3	39.7	35.2	47.6	50.0
0.7	42.2	41.9	39.4	35.5	46.7	48.5
$x_p$	42.8	42.7	38.5	38.4	47.7	49.4

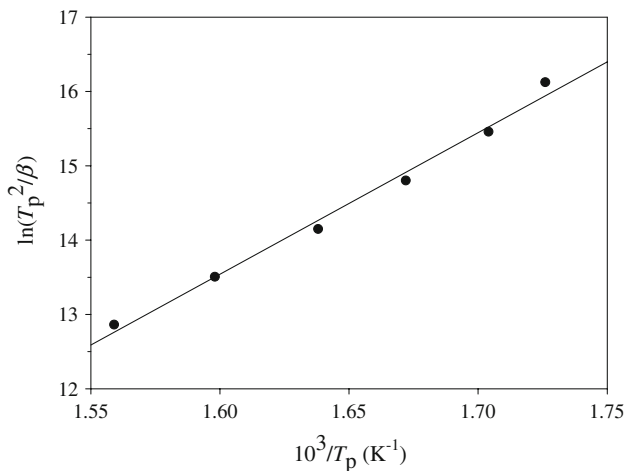


**Fig. 7** Plots of  $\ln(T_p^2/\beta)$  vs.  $10^3/T_p$  and straight regression line of the  $\text{Sb}_{0.12}\text{As}_{0.40}\text{Se}_{0.48}$  alloy ( $\beta$  in  $\text{K s}^{-1}$ )

**Table 6** Kinetic parameters calculated by the procedure described in section “Basic theory” and by maximum-value technique

Alloy	Technique	$E$ (kcal mol $^{-1}$ )	$n$
S1	Object of this work	40.5	2.9
	Maximum-value	41.1	2.8
S2	Object of this work	38.0	2.0
	Maximum-value	38.1	1.9
S3	Object of this work	46.8	2.4
	Maximum-value	43.6	2.3

depend on the mechanism of nucleation and growth and the dimensionality of the crystal. In addition,  $n = m + 1$  for a quenched glass containing no nuclei whilst  $n = m$  for a glass containing a sufficiently large number of nuclei. The kinetic parameters have been deduced by using the following considerations: the condition of the maximum crystallization rate and the quoted maximum rate. The theoretical procedure has been applied to the crystallization kinetics of some glassy alloys, prepared in our laboratory, as-quenched and previously reheated. According to the study carried out, it is possible to establish that the reheating did not cause the appearance of nuclei, but that the three as-quenched alloys fulfil the condition of “site saturation”. These alloys have been also analysed by means of the maximum-value technique, finding that the error between the values of the kinetic parameters obtained by both procedures is less than 6.8%. This good agreement shows the reliability of the theoretical procedure developed for the calculation of the kinetic parameters in materials

involving nucleation and crystal growth processes, which occur in separate stages.

**Acknowledgements** The authors are grateful to the Junta de Andalucía (PAI/EXCEL//FQM0654) and the Spanish Ministry of Science and Education (MEC) (Project No. FIS2005-01409) for their financial supports.

## References

- Liu F, Sommer F, Mittemeijer EJ (2004) *J Mater Sci* 39:1621. doi:10.1023/B:JMSS.0000016161.79365.69
- Zhu JQ, Bo ZL, Dong DK (1996) *Phys Chem Glasses* 37:264
- Abdel-Rahim MA, Ibrahim MM, Dongol M, Gaber A (1992) *J Mater Sci* 27:4685. doi:10.1007/BF01166006
- Weinberg MC, Kapral R (1989) *J Chem Phys* 91:7146
- Vázquez J, Villares P, Jiménez-Garay R (1997) *J Alloys Compd* 257:259
- Frade JR (1998) *J Am Ceram Soc* 81:2654
- Ray CS, Fang X, Day DE (2000) *J Am Ceram Soc* 83:865
- López-Alemán PL, Vázquez J, Villares P, Jiménez-Garay R (2003) *Mater Lett* 57:2722
- Johnson WA, Mehl KF (1939) *Trans Am Inst Mining Met Eng* 135:416
- Avrami M (1939) *J Chem Phys* 7:1103
- Avrami M (1940) *J Chem Phys* 8:212
- Avrami M (1941) *J Chem Phys* 9:177
- Kissinger HE (1957) *Anal Chem* 29:1702
- Ozawa T (1970) *J Thermal Anal* 2:301
- Henderson DW (1979) *J Non-Cryst Solids* 30:301
- Moharram AH, Abu El-Oyoun M, Abu-Sehly AA (2001) *J Phys D Appl Phys* 34:2541
- Donald IW (2004) *J Non-Cryst Solids* 345 and 346:120
- Kozmidis-Petrović AF, Štrbac GR, Štrbac DD (2007) *J Non-Cryst Solids* 353:2014
- Fine ME (1964) *Introduction to phase transformation in condensed system*, chap 3. Macmillan, New York
- Cahn JW (1956) *Acta Metall* 4:572
- Cahn JW (1956) *Acta Metall* 4:449
- Matusita K, Komatsu T, Yokota R (1984) *J Mater Sci* 19:291. doi:10.1007/BF00553020
- Kolmogorov AN (1937) *Bull Acad Sci USSR (Sci Mater Nat)* 3:3551
- López-Alemán PL, Vázquez J, Villares P, Jiménez-Garay R (2000) *J Non-Cryst Solids* 274:249
- Shneidman VA, Uhlmann DR (1998) *J Chem Phys* 109:186
- Yinnon H, Uhlmann DR (1983) *J Non-Cryst Solids* 54:253
- Christian JW (1975) *The theory of transformations in metals and alloys*, 2nd edn. Pergamon Press, New York
- Vázquez J, Wagner C, Villares P, Jiménez-Garay R (1996) *Acta Mater* 44:4807
- Gao YQ, Wang W (1986) *J Non-Cryst Solids* 81:129
- Vázquez J, López-Alemán PL, Villares P, Jiménez-Garay R (1998) *Mater Chem Phys* 57:162
- Vázquez J, López-Alemán PL, Villares P, Jiménez-Garay R (1998) *J Alloys Compd* 270:179
- Sestak J (1974) *Phys Chem Glasses* 6:137